ETH
Eidgenössische Technische Hochschule Zürich
Swiss Federal Institute of Technology Zurich

Semi-supervised learning using Total variation for biomedical image segmentation

Master Thesis

Prateek Purwar

Department of Electrical Engineering and Information Technology

Advisor: Dr. Gregory Paul

Supervisor: Prof. Dr. Orcun Goksel

Abstract

Image segmentation is a fundamental middle-level computer vision task, necessary to higher level image understanding, such as semantic image analysis, scene understanding, diseases diagnosis, etc. Recently, convolutional neural networks (CNN) have set new state-of-the-art standards in the field, and attract a lot of attention among both practitioners and experts. Beyond the accuracy they can achieve in many computer vision tasks, their attractivity lies in their versatility, their capability to be reused and transferred to similar problems, their layered architecture, and their capability to learn meaningful features. Nonetheless, in practice, the main obstacle is to obtain a sufficient number of annotated image data for the task at hand.

This poses a major problem for application scenarios where large annotated data-sets are not available or difficult to obtain. This thesis tackles such a case, and is motivated by the problems faced in an imaging facility: annotations can be difficult, even for experts, images are very diverse in nature, and in appearance.

In this thesis, we tackle the problem of applying CNNs in a semi-supervised and semi-interactive image segmentation scenario. We study how the segmentation accuracy of a segmentation pipeline evolves with the annotation effort of the user. Our base CNN is OSVOS, developed for video segmentation, where only a very small subset needs to be annotated (one to three frames fully labeled). This work focuses on partially annotated images with scribbles. We compare two strategies: a random forest (RF)-based and CNN-based. We derive a loss function for training CNNs from scribbles. Varying amounts and different types of scribbles are used to train either a RF or our modified OSVOS. We show that both the quantity and quality of the annotations are important for increasing the segmentation accuracy, and that the RF-based pipeline is better for the low-annotation regime.

We also compare different post-processing strategies of the predicted soft segmentation mask: thresholding and variational image segmentation. We show that the type of labeling cost used in the variational

model matters. The model we propose ensures that one can always benefit from post-processing the soft-mask with a variational method. This is not the case for the widespread cost function in the literature, that can degrade the segmentation accuracy, even when the RF or the CNN make good predictions.

Acknowledgements

I would like to acknowledge the support of my Master Thesis advisor Dr. Gregory Paul, Post-Doc. at Computer Vision Laboratory at ETH. I would like to thank Jordi Pont-Tuset for steering me in right direction whenever I got stuck. I would sincerely thank Denis Samuylov and Christoph Mayer, who helped with implementation and coding at each step of my thesis.

Contents

List of Figures

Chapter 1

Introduction

The task of image segmentation into binary classes is very useful in different cases in biomedical tasks. It can be used for detection of diseases, shape analysis etc. The methods to solve the segmentation problem has evolved along two lines: 1) level of interaction: from semi-interactive to fully automatic, and 2) level of classification: pixels to complete images. Nowadays, with the use of fully-convolutional networks, the segmentation can be obtained for a complete image in one forward pass. This helps in using the local as well as contextual information for segmentation. Currently, the benchmark performance in terms of accuracy is achieved by the use of convolutional neural networks (CNN). The neural networks are specialized to learn feature maps from the examples provided and specific to the task at hand. These networks require a huge amount of training data: images and ground truth i.e. label for each pixel in the input image; to train the network from scratch. In literature, we can find different architectures of neural networks specially designed for the task of segmentation, one of the popular architecture is U-Net [1]. This approach works well for tasks where we can find a significant number of images and can train a neural network. However, this poses a difficulty when we are trying to segment objects in microscopic images.

1.1 Electron Microscopy Images

The dataset which we are trying to segment is electron microscopic (EM) images of liver tissue. The dataset consists of a 3D stack of 2D slices of liver tissue as shown in figure 1.1. The dataset can be considered as a single 3D stack or multiple 2D slices for our task. We can observe following traits in EM images:

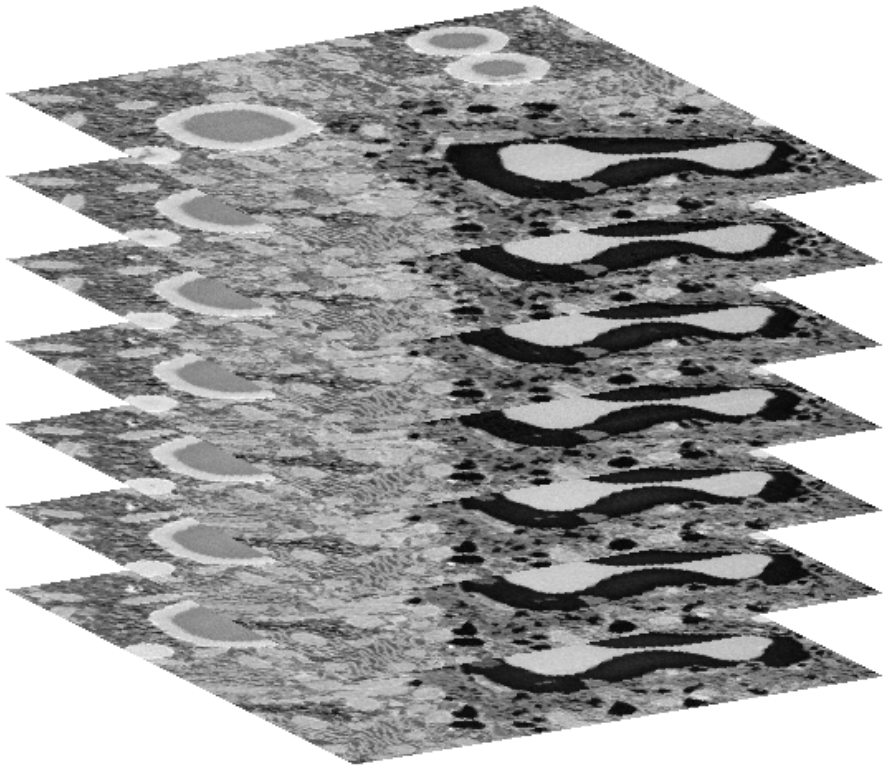

Figure 1.1: A 3D image stack, output from a scanning electron microscope. The stacks contains 458 2D images with a resolution of 1890x1952 pixel each.

- High variability between images: The images to be segmented may be entirely different i.e. having fixed objects as in liver tissue or having layers to segments as in neuron tissue. The objects to be segmented may differ completely from being smooth (round vesicles) to branched (neurons). This prohibits the use of one dataset to train a network for another dataset and thus, restricting the availability of images.

- High variability between objects to segment: The objects to be segmented vary significantly in shape, size, and texture in different images. We can observe few objects of interest in figure 1.2.

- High variability between goals: Even for a single image, the goal of the segmentation can be totally different. The images annotated for one object can not be used again for training purpose.

These characteristics of EM images make it very difficult to fully annotate each object of interest and is extremely time-consuming for experts. Here for our task, we are interested to segment vesicles, as shown in figure 1.3. The difficulty in annotating different vesicles of undefined shapes and sizes can be observed

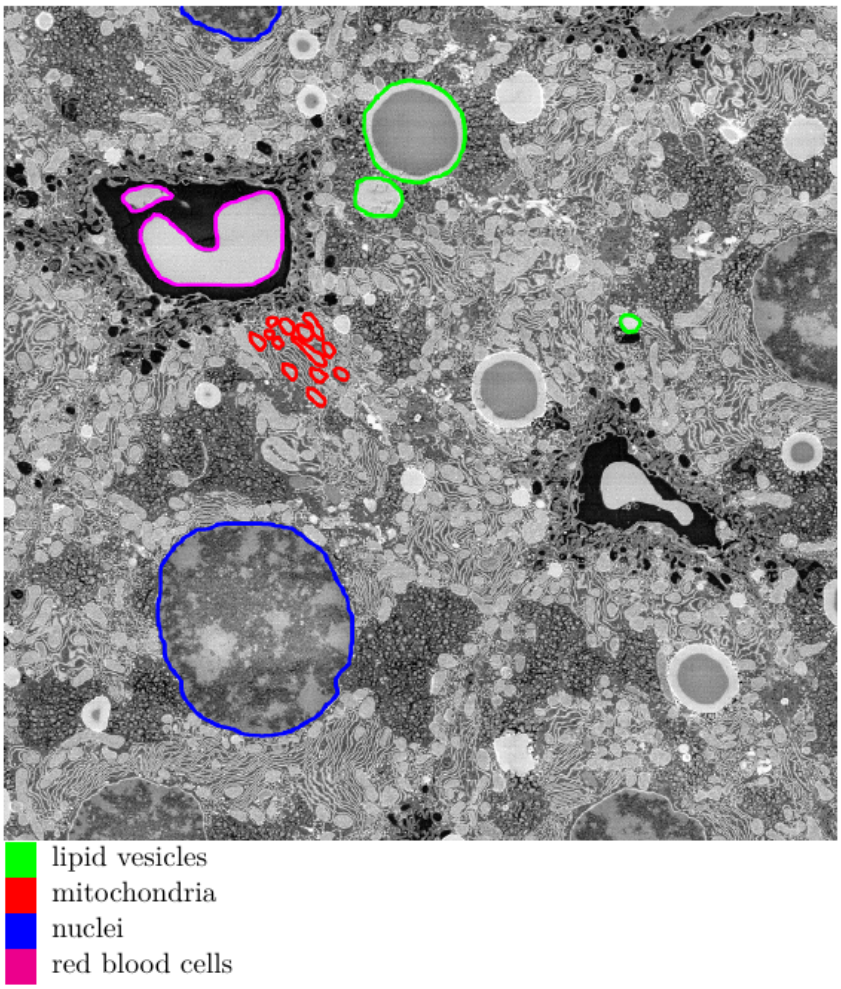

Figure 1.2: Example of Manual annotations of different objects in liver tissue.

in Figure 1.3. To add to this complexity, the experts are uncertain about the existence of vesicles in certain parts of images and sometimes, even one expert annotates differently at different times. The difference in annotations can be observed for different experts and also for annotations of the same image by the same expert, as shown in figure 1.4. For example, we can observe differences in rectangular boxes in figure 1.4. This uncertainty has been analyzed in literature and researchers have tried to come up with different methods to get one ground truth mask from these multiple annotations by experts. We can use STAPLE [2] algorithm or union or majority voting to derive reference mask. The reference mask derived for one slice using STAPLE and union is shown in figure 1.5

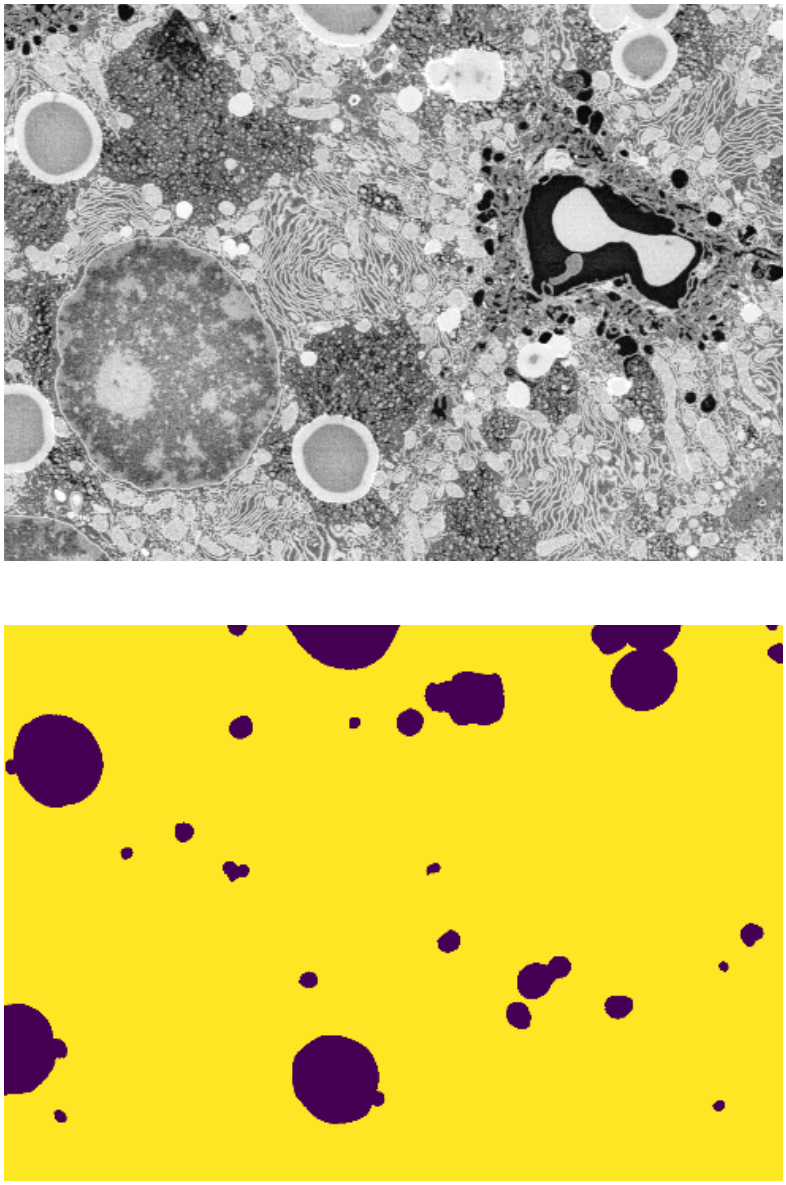

Figure 1.3: Cropped part of slice 15 and its ground truth annotation by an expert.

1.2 Focus of this thesis

Nowadays, it is common to train deep neural networks (DNN) using transfer learning to compensate for the lack of enough data for training. Recently, Shelmar et al. [3] designed a ”fully convolutional” network that takes input of arbitrary size and produces segmented output for a complete image. They adapted contem-

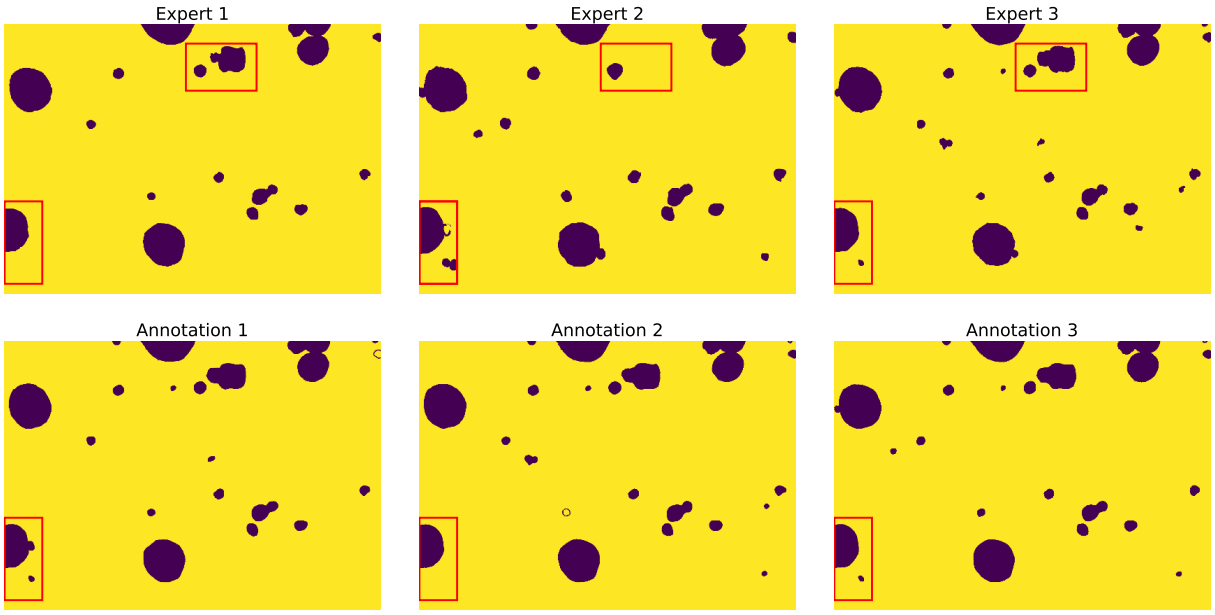

Figure 1.4: Upper row: Annotation of an slice by different experts. Bottom row: Multiple annotations of an slice by same expert. One example of difference can be observed in bounding boxes.

porary classification networks (AlexNet, the VGG net, and GoogLeNet) into fully convolutional networks and transfer their learned representations by fine-tuning to the segmentation task. Similar to this, we use and fine-tune network explained in Caelles et al. [4]. This paper tackles the task of **semi-supervised** video object segmentation, i.e., segment an object in a video, given fully annotated mask of the object in the first frame. This task can be considered to be similar to segmenting objects in a 3D stack of slices. We try to fine-tune the network using fully annotated objects in few slices in the stack. We describe the details and observations in Section 2.

Figure 1.5: Grounth truth mask derived from multiple annotaions using 2 different methods

The use of pre-trained networks makes it possible to use DNN even with small amount of training data. But still to train the DNN, we need to provide fully annotated masks for objects of interest for all training images and this comes out to be a tedious and difficult task as explained above. In addition, the presence of multiple objects of different shape and sizes makes it even more difficult and time-consuming. Imagine 1000 cells in a 2D slice and possibility to manually annotate all these cells of undefined shapes! This provides us with the option of annotating few objects and train networks using either cropped images or treating rest of image as background. Or we can use semi-supervised learning using partial annotations. In literature, we can find various methods to use these partial annotations to classify each pixel as foreground or background. For example, Santner [5] describes the use of Random forests (RF) for image segmentation using partial annotations. In this thesis, we try to discover the effect of annotation budget i.e. the number of pixels to annotate and the accuracy achieved. We also try to learn which pixels to annotate to use our annotation budget efficiently.

These methods only learn pixel level information and are uncertain for the maximum of pixels i.e. the probability of foreground learned is not binary but lies between 0 and 1. In literature, different approaches can be found to use prior information to compensate for data and for the uncertainty of estimators. The most common are to use Conditional random fields (CRFs) or graph cuts to regularize the probability learned. We solve this problem using a prior in **Bayesian framework**. Santner [5] uses a weighted total variation as prior and Random forests to learn likelihood. Ranftl [6] uses CNN to learn unary and edge potential and combine this information to get segmentation mask using graph cuts. For our task, we implement the method described in the master thesis of Eugster [7]. In Eugster [7], they try to learn likelihood using Random forests and prior as an isotropic total variation (TV). They use a non-linear cost function to formulate likelihood from probabilities learned from Random forests. This is quite different to the common approach of using probabilities directly as likelihood to combine with prior. A majority of researchers using CNN use a linear cost function to implement prior with help of CRFs. In this thesis, we analyze and compare these different cost functions. We try to observe the advantage of using these cost functions in different scenarios. For images as 3D stacks, it is observed to be a difficult task and computationally efficient to encode 3D information in models as CNN or RF for learning likelihood. Also, it is common practice to use prior information in 2D. Thus, we also try to observe benefits of using 3D isotropic total variation in case of 3D

stacks.

In summary, we use a Bayesian approach with RF to parametrize likelihood and isotropic TV as prior to predict segmentation mask for a given image. This gives us chance to generate fully annotated segmentation masks and train CNN to obtain better accuracy. The common problem for use of prior is the choice of appropriate scaling to couple likelihood and prior costs. Ranftl [6] coupled the prior cost function with the likelihood cost function obtained from CNN. They optimized the final loss function to obtain optimal values for network parameters (weights and biases) and regularization parameter. Riegler [8] [9] proposed a method to implement TV as specialized layers in CNN and trained the complete model, CNN + TV, together. This motivated us to replace RF with CNN and try to learn pre-trained fully convolutional network from partial annotations. We were able to restructure cross-entropy loss to compute loss for partial annotations.
Finally, we also showed the advantage of using iterative semi-interactivity for efficient use of annotation budget and also to be able to provide an opportunity to experts to improve learning method according to their specific requirements.

1.3 Thesis Organization

The thesis is divided mainly into two sections: segmentation using fully annotated objects and segmentation using partial annotations. The segmentation using full annotations is described in Section 2. The latter method is described in Section 3. In section 3.1, we describe the improvement in segmentation mask for increased labeling effort. We introduce the use of prior and variational methods in section 3.2. In section 3.3, we introduce use CNN to learn from partial annotations. Finally, in the last section, we conclude this thesis and lay out future work that can be done.

Chapter 2

Fully annotated segmentation masks

The deep neural networks have become popular to solve any task in the field of computer vision. To train a network from scratch, the main effort goes into preparing data for training network, and in coming up with the best architecture and choosing best training parameters. The data is available on the internet and can be extracted and modified for various tasks such as IMDB database can be used to train network for the problem involving faces. This becomes a problem in the medical domain where it is very costly to generate images and even more costly and time-consuming to prepare it for training. For our problem of image segmentation, we described the problem faced by experts and researchers in generated segmented masks. The lack of data has motivated researchers to use transfer learning. Transfer learning tries to store the knowledge gained from solving one problem and applying it to a different but related problem. Thus, in practice, it is very rare to train an entire Convolutional Network from scratch (with random initialization), because it is relatively rare and difficult to have a dataset (images and labels) of sufficient size for training. Instead, it is common to use a pre-trained network either to initialize a network or to extract required feature maps. We decided to use pre-trained network and fine-tune it for our task.

2.1 One shot Video object segmentation (OSVOS)

Caelles et al. [4] designed an architecture to segment an object in a video sequence using only one frame for training. The network is trained to learn object from only one frame and generate segmentation mask for remaining all frames. The segmentation works well if the object remains in relatively similar shape and

size. This can be considered similar to our problem of segmenting vesicles in the 3D stack of liver tissue. Since the vesicles are relatively similar in shape and size in different slices, we annotated first few slices to train the network. We generated more data using cropped and flipped slices for training. In literature, we can find that network can overfit on a relatively small dataset. The use of augmentation helps in generating more data and avoids network from overfitting.

OSVOS uses pre-trained network of VGG-net for initialization. They removed the final fully-connected layers and replaced them with deconvolution layers to generate a mask of image size. In addition, the network contains end output, side outputs and main output generated from a combination of side outputs. They also these side outputs to segment retinal nerves in Maninic et al. [10]. The total loss is calculated for all outputs and used for backpropagation. The details of architecture and initialization parameters can be found in Caelles et al [4]. As we described the difficulty of annotating full objects in Section 1, we tried to observe accuracy improvement with the increase of training data. We trained OSVOS from 1 slice and increased the training data to 10 slices. The initialization parameters were kept same for cases. In figure 2.1, we can observe that OSVOS performs well with only 2 slices. The segmentation output from CNN trained using 2 slices is also shown in figure 2.1.

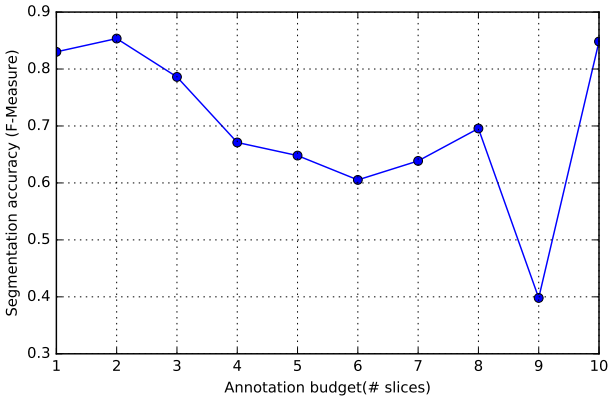

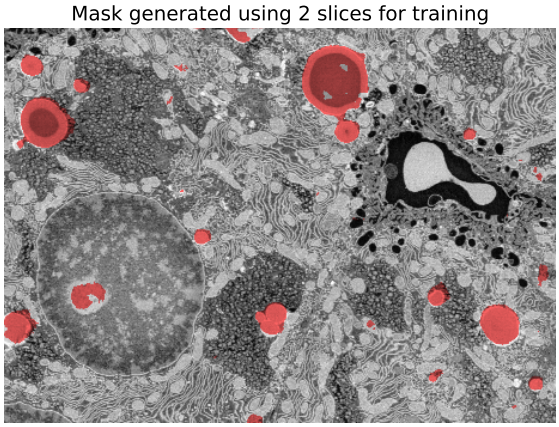

Figure 2.1: Left image: F-measure computed for different amount of training data; Right image: Predicted mask for one slice

We expected increase in performance with the increase in the amount of data. This does not happen as CNN is not able to converge equivalently for all cases. It is important to remember here that annotating one slice is not same as one object. We can observe these multiple objects in figure 1.2. Also, change

in annotation will force us to train network again. These difficulties motivated us to try semi-supervised learning for our task of segmentation.

Chapter 3

Semi-supervised image segmentation

The philosophy behind semi-supervised learning is to propagate label information from labeled to unlabeled data. Image segmentation can be seen as a classification problem which consists of assigning a class label to each pixel. For our task of binary segmentation, this means classifying each pixel as foreground or background. For our task of image segmentation, we make use of partial annotations as *scribbles*. Scribbles are pixels in image annotated by experts as foreground or background. We use example-based methods to learn from these scribbles annotated by experts. In contrast to having different images for training and testing, we use same image for training and testing as the samples used for training are pixels and not images.

3.1 Random Forest

In this section, we make use of random forest (RF) as the semi-supervised learning algorithm. The advantages and details of using RF can be found in Eugster. For training RF, we compute set of features in Python. We compute different features ranging from simple Sobel edge detectors to higher level Gabor filters. The choice of features was made according to WEKA [11] toolset of FIJI [12] plugin. These are set of 2D features and perform well for medical images. We compute the different type of features for a range of sigmas, which gives 69 feature maps for a single image. In the thesis by Eugster [7], we can find details and effect of feature selection for training Random forests. As shown in figure 3.1, we can observe that for given annotation budget, the segmentation measure does not change significantly for more than 30 trees and for more than 20 features. Therefore, for all experiments using RF, we use 20 best features and 30 trees for

training. In this thesis, we focus on how to get best results for given annotation budget and thus, use fixed number of features and trees to generate masks. We try to answer the question of where to scribble and how to make the best use of our annotation budget and time.

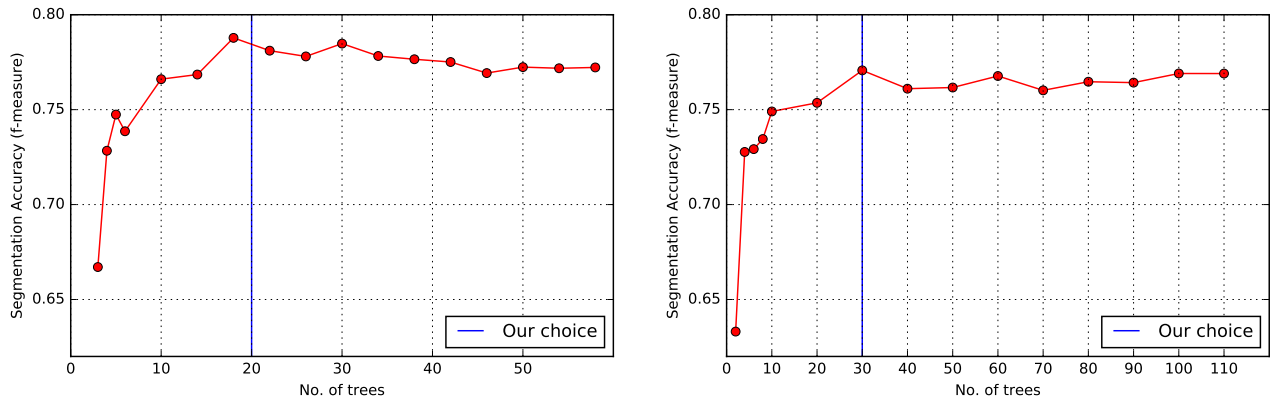

(a) (b)

Figure 3.1: Plot of segmentation measure vs changing complexity of RF: (a) with features, (b) with trees

3.1.1 Where to scribble?

In general, we believe that the more training data we provide, more we can improve the results. Does this hold for partial annotation such as scribbles? If we go on increasing the pixels annotated arbitrarily, will it improve the segmentation mask or we have to use our labeling effort intelligently to improve results? We conducted an experiment by dividing our set of foreground and background scribbles into 2 classes: easy and hard. We classified scribbles as ”easy” and ”hard” depending on the effort required to annotate these pixels. For example, pixels are difficult to annotate near the boundary of foreground and background, and we classify these pixels as ”hard”, as shown in figure 3.2. We manually scribbled image for both ”easy” and ”hard” subclasses. Then, we trained and tested RF on one image by increasing percentage of scribbles belonging to ”easy” foreground and background class. After we have used all scribbles belonging to ”easy” class, we added scribbles from ”hard” class for both foreground and background. The increment was done w.r.t. the total amount of scribbles we are having and also, for a higher percentage of added scribbles, we maintained a ratio between foreground and background pixels. The result can be observed in figure 3.3(a).

In figure 3.3(a), we can observe that after a total of 3000 pixels selected from ”easy” foreground and background, the segmentation measure does not change significantly. An improvement can be observed,

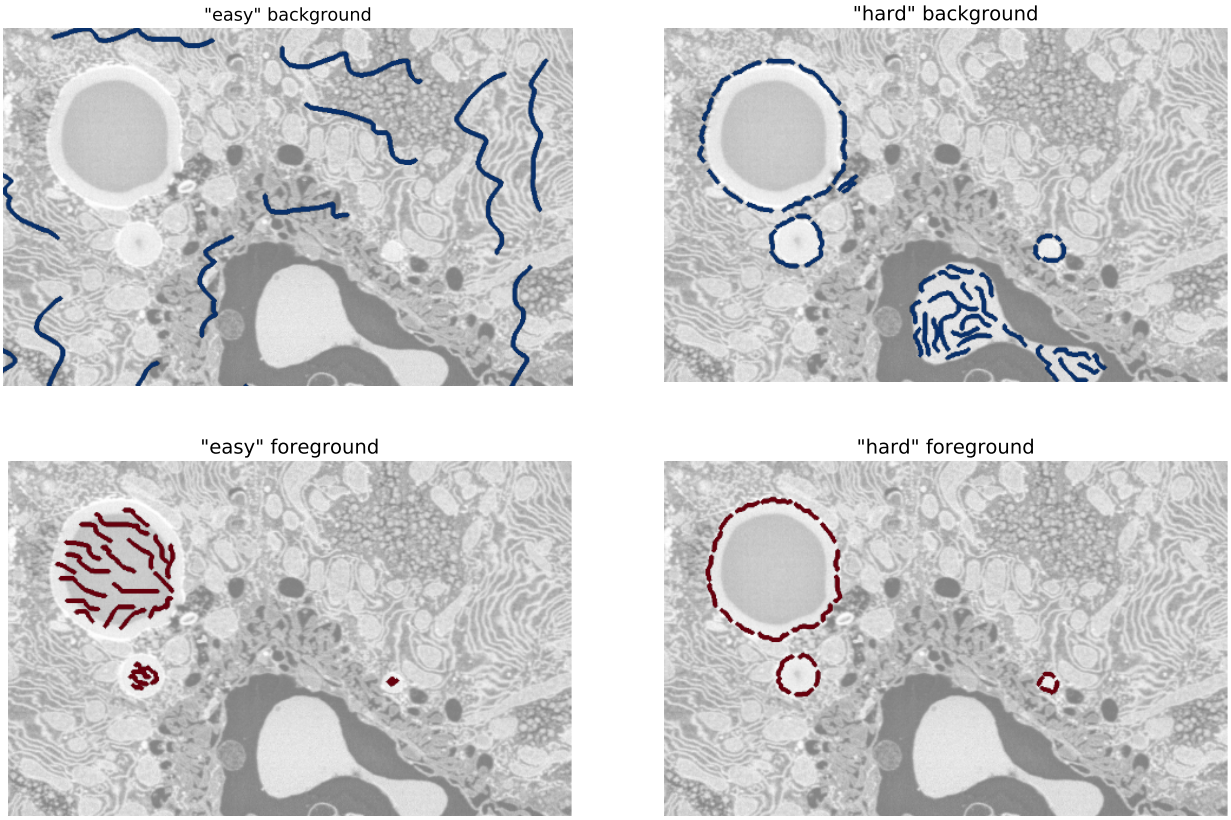

Figure 3.2: Manual scribbles in ”easy” and ”hard” classes

once we started adding ”hard” scribbles after all ”easy” scribbles were used. This shows that the best results can be obtained by adding ”hard” scribbles after addition of a certain percentage of ”easy” scribbles. Looking at the plot, one might think to start adding the ”hard” scribbles after 3000 ”easy” scribbles. We tried this and results can be observed in figure 3.3(b).

In figure 3.3(b), as we started adding ”hard” scribbles on top of 10% (3000 pixels) of scribbles selected from ”easy” scribbles, instead of observing a rise with additional scribbles, we observed a fall in performance (dark blue plot in figure 3.3(b)). This may be due to lack of enough ”easy” scribbles and RF starts training its trees to focus more on ”hard” scribbles. We tried a similar experiment with the different amount of ”easy” scribbles to start with. We started seeing a significant improvement when we utilized with 70% of all ”easy” scribbles to train RF. We were able to achieve f-measure score of 0.83 in comparison of 0.84 achieved with 100% usage of ”easy” scribbles (See green and pink plot in figure 3.3(b)). Thus, the question arises how to decide the point of addition of ”hard” scribbles.

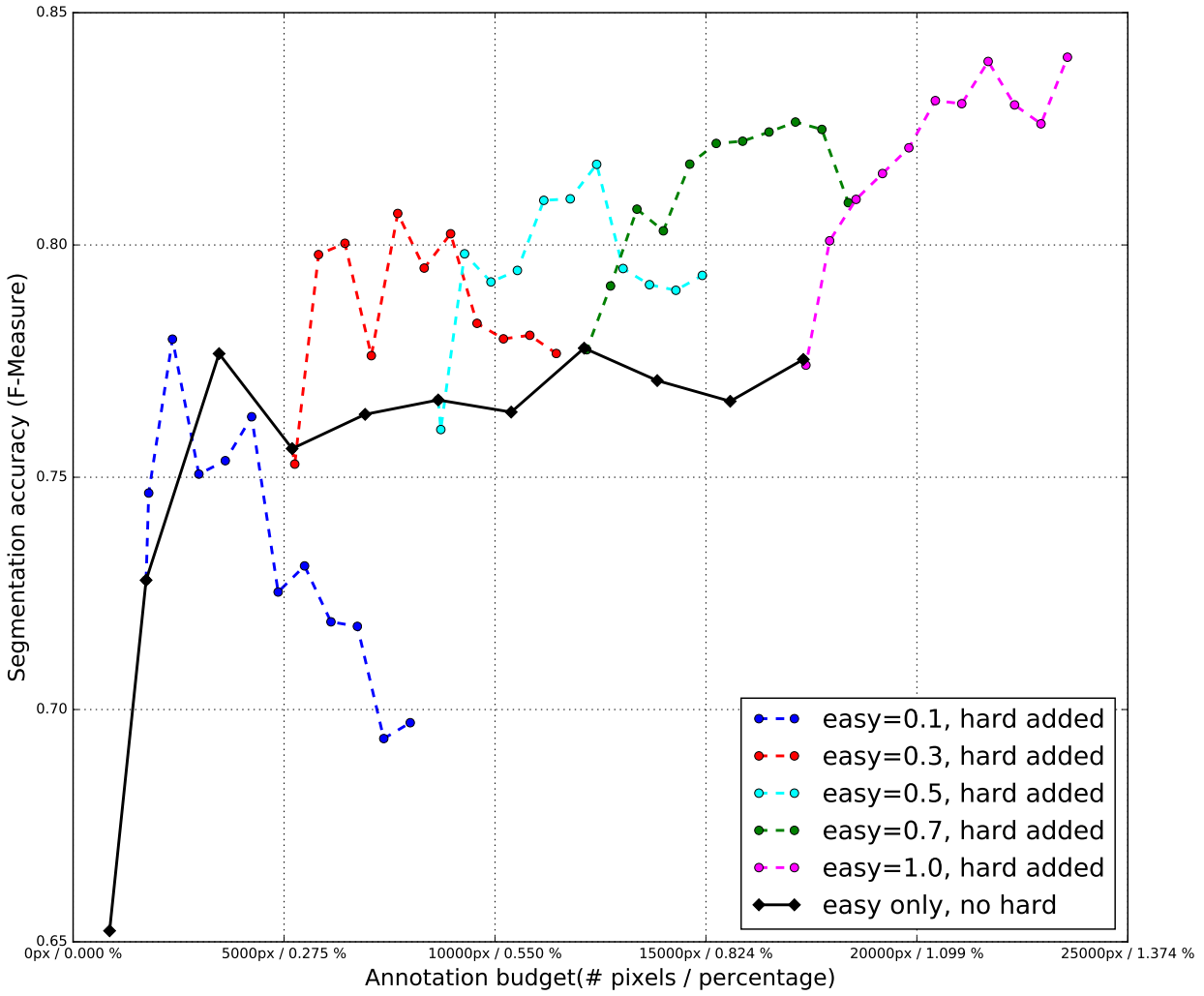

Figure 3.3: Plot of segmentation measure vs annotation budget. The black curve shows change in segmentation measure with increment of scribbles from ”easy” class. Other curves and show change in segmentation measure with increment of scribbles from ”hard” class, starting with different fixed amount of ”easy” class.

3.1.2 Iterative semi-interactive approach

In the previous section, we showed the need of using our annotation budget intelligently to get the best performance. But, we observed the problem of deciding on how many ”easy” and ”hard” scribbles are needed to achieve best results. For our problem, we divided the scribbles as ”easy” and ”hard” according to labeling effort, but this division for scribbles may not be same from point of view of the Random forest. Apriori, we don’t know which pixels will be difficult for the Random forest to classify correctly. The above mentioned two problems can be solved by annotating pixels iteratively to improve results, at least once to

understand which pixels are difficult for RF to classify. We show the improvement in the result by doing one iteration in figure 3.4. We can observe that the scribbles are very few to produce a good result. Still, we can observe improvement in f-measure from 0.745 to 0.749 for increasing the annotation budget from 7500 pixels to 10900. Although the increment looks insignificant, but we can observe the difference in the large vesicle in left-top corner of the image.

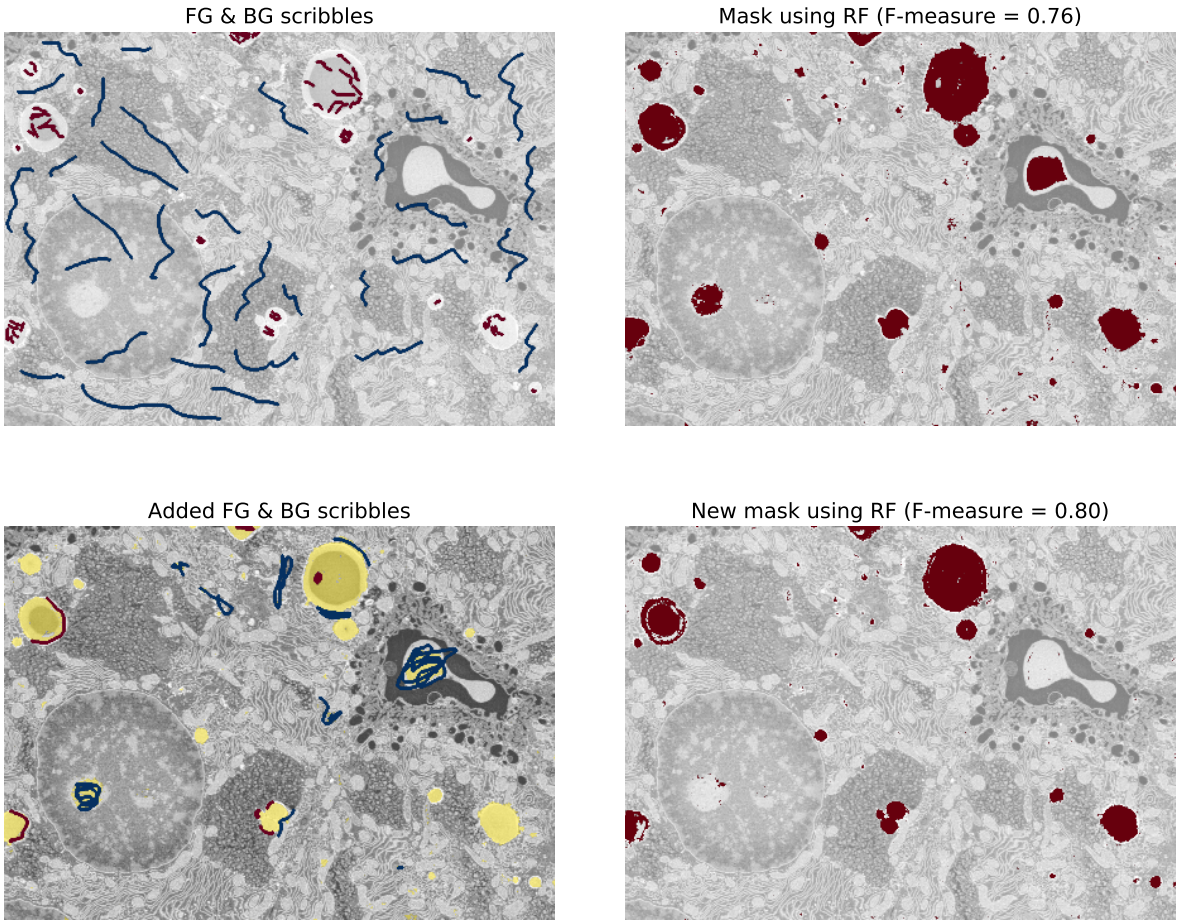

Figure 3.4: Semi-interactive segmentaion with one iteration

3.1.3 Uncertainity of classifier

The use of iterative semi-interactivity gives the best result for given annotation budget, but the output of RF is noisy and uncertain. The uncertainty lies in the inability to classify maximum of pixels as foreground and background, as shown in figure 3.5(a). The histogram shows the distribution of probability values for the

complete image. It can be seen that a large number of pixels are not given a probability of 0 (background) or 1 (foreground). In figure 3.5(b), we can observe varying results for different threshold applied on output from RF. RF acts as a classifier and classifies each pixel but we need to group these pixels into objects for segmentation. In this thesis, we make use of prior information to compensate for the lack of enough annotated data and for the uncertainty of classifier.

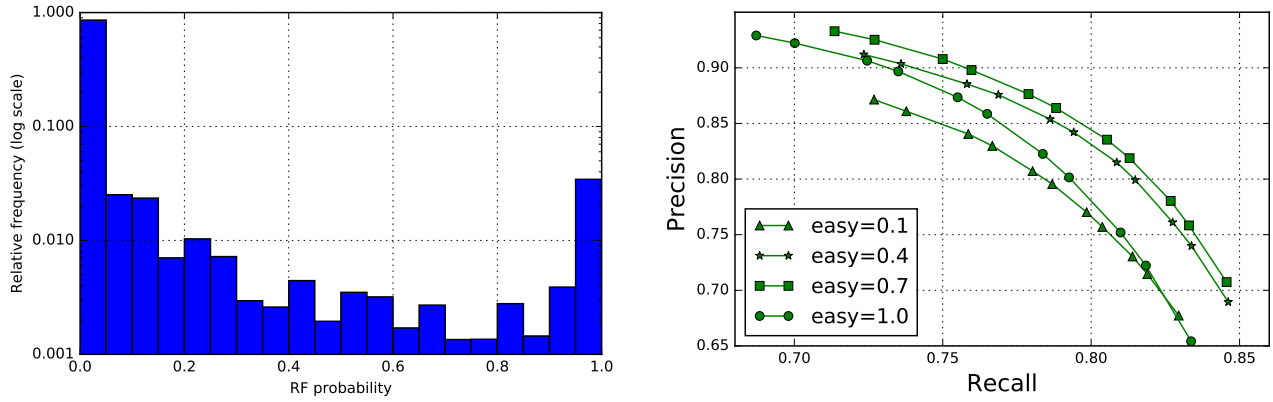

(a) (b)

Figure 3.5: (a) Histogram of probabilities. (b) Precision-recall curve for varying thresholded RF mask. Different curves for different annotation budget

3.2 Bayesian Formulation

To make use of prior, we model our image segmentation problem as a Bayesian inference problem. Let us cosider an observed image, $\boldsymbol{I}$ and labeled or segmented ground truth, $\boldsymbol{M}$, the joint probabilty can be defined as:

$$\boldsymbol{p}(\boldsymbol{I}, \boldsymbol{M}) = \boldsymbol{p}(\boldsymbol{M})\boldsymbol{p}(\boldsymbol{I}|\boldsymbol{M}) \quad ,$$

and applying Bayes theorem,

$$\boldsymbol{p}(\boldsymbol{M}|\boldsymbol{I}) = \frac{\boldsymbol{p}(\boldsymbol{M})\boldsymbol{p}(\boldsymbol{I}|\boldsymbol{M})}{\boldsymbol{p}(\boldsymbol{I})}$$

$$\alpha\, \boldsymbol{p}(\boldsymbol{M})\boldsymbol{p}(\boldsymbol{I}|\boldsymbol{M})$$

The left hand side is the probability of obtaining segmentation mask, $\boldsymbol{M}$ given the image $\boldsymbol{I}$, is called the posterior probability. $\boldsymbol{p}(\boldsymbol{M})$ is the prior probability of mask, $\boldsymbol{M}$. The Maximum a posteriori (MAP) estimate, $\boldsymbol{M^*}$ can be calculated as follow:

$$\boldsymbol{M^*} = \arg\max_{\boldsymbol{M}}(\boldsymbol{p}(\boldsymbol{M})\boldsymbol{p}(\boldsymbol{I}|\boldsymbol{M})) \quad . \tag{3.1}$$

The above problem can as well be stated as an energy minimization problem by writing Equation 3.1 in terms of energy by taking negative log-likelihood:

$$\begin{aligned} E(\boldsymbol{M}) &= -\log(\boldsymbol{p}(\boldsymbol{I}, \boldsymbol{M})) \\ &= -\log(\boldsymbol{p}(\boldsymbol{I}|\boldsymbol{M})) - \log(\boldsymbol{p}(\boldsymbol{M})) \\ &= E_d(\boldsymbol{I}, \boldsymbol{M}) + E_r(\boldsymbol{M}) \end{aligned}$$

The total energy, E, that we want to minimize can be considered as linear combination of data or likelihood term, E_d and prior term (or regularization), E_r. This modifies calculating MAP estimate to:

$$\boldsymbol{M^*} = \arg\min_{\boldsymbol{M}}(E_d(\boldsymbol{I}, \boldsymbol{M}) + E_r(\boldsymbol{M})) \quad .$$

To obtain MAP estimate, we need to formulate likelihood term and prior term. We formulate the prior using Total variation(TV). We can find use of different TV priors such as Wulff shapes etc. In our thesis, as the objects we need to segment are smooth and shaped like a circle, we make use of isotropic total variation, TV. Also, we can try to use isotropic total variation in 2D and 3D as the data we are trying to segment is a 3D stack. For likelihood term, G. Paul et al.[13] proposed an energy formulation which is not derived from a statistical model but learnt from training set. This gives the advantage of combining example-based and model-based approaches. Similar to Eugster [7], we formulate the likelihood term as product term of a cost function, C, of soft mask, $\boldsymbol{P}$(probability of each pixel being foreground) learnt from RF and optimal mask

to be estimated, $\boldsymbol{M}$. The energy minimization problems becomes:

$$\begin{aligned} E(\boldsymbol{M}) &= E_d(\boldsymbol{I}, \boldsymbol{M}) + E_r(\boldsymbol{M}) \\ &=< C(\boldsymbol{P}), \boldsymbol{M} > +\lambda\ TV(\boldsymbol{M}) + \mathrm{i}_{[0,1]}(\boldsymbol{M}) \quad , \end{aligned}$$

where $\mathrm{i}_{[0,1]}(\boldsymbol{M})$ is an indicator function to ensure values of $\boldsymbol{M}$ remain in [0,1]. In addition to use of cost function, we enforce constraint of preserving the pixels annotated by experts as foreground and background in our energy minimization problem. We used an indicator function, $\mathrm{i}_{fg}(\boldsymbol{M})$, to ensure pixels in foreground scribbles have value of 1 in mask, and indicator function, $\mathrm{i}_{bg}(\boldsymbol{M})$, to ensure pixels in background scribbles have value of 0 in mask. Using discrete implementaion of TV, the final energy minimization problem is formulated as given below:

$$E(\boldsymbol{M}) =< C(\boldsymbol{P}), \boldsymbol{M} > +\lambda \, \| |\boldsymbol{D}\boldsymbol{M}|_2 \|_1 + \mathrm{i}_{[0,1]}(\boldsymbol{M}) + \mathrm{i}_{fg}(\boldsymbol{M}) + \mathrm{i}_{bg}(\boldsymbol{M})$$

The optimization problem is solved using Alternating Split Bregman method (ASB), as described in Eugster [7]. The advantage of using ASB is that it splits the above problem into subproblems. Each subproblem is easy to solve and can be solved independently. The final solution to the problem is obtained by iterating updates. The details of implementation and solution can be obtained from Eugster [7]. The results for RF with variational segmentation (with ***anti-nll*** cost function described in following section) can be seen in figure 3.6. We can observe different improvement due to the use of the variational method for different regularization parameter (λ). The boost obtained from variational image processing (VIP) with best among different λ can be seen in figure 3.7. The advantage can be seen that the boost is always positive implying that use VIP never degrades the performance of RF. In the following section, we describe and compare the use of different cost functions in Variational segmentation methods.

3.2.1 Different likelihhood formulations

In literature, people have formulated the cost function either directly using the soft mask ($\boldsymbol{P}$) obtained from RF or, some linear or non-linear function of the mask. Santner [5] formulates likelihood term as linear

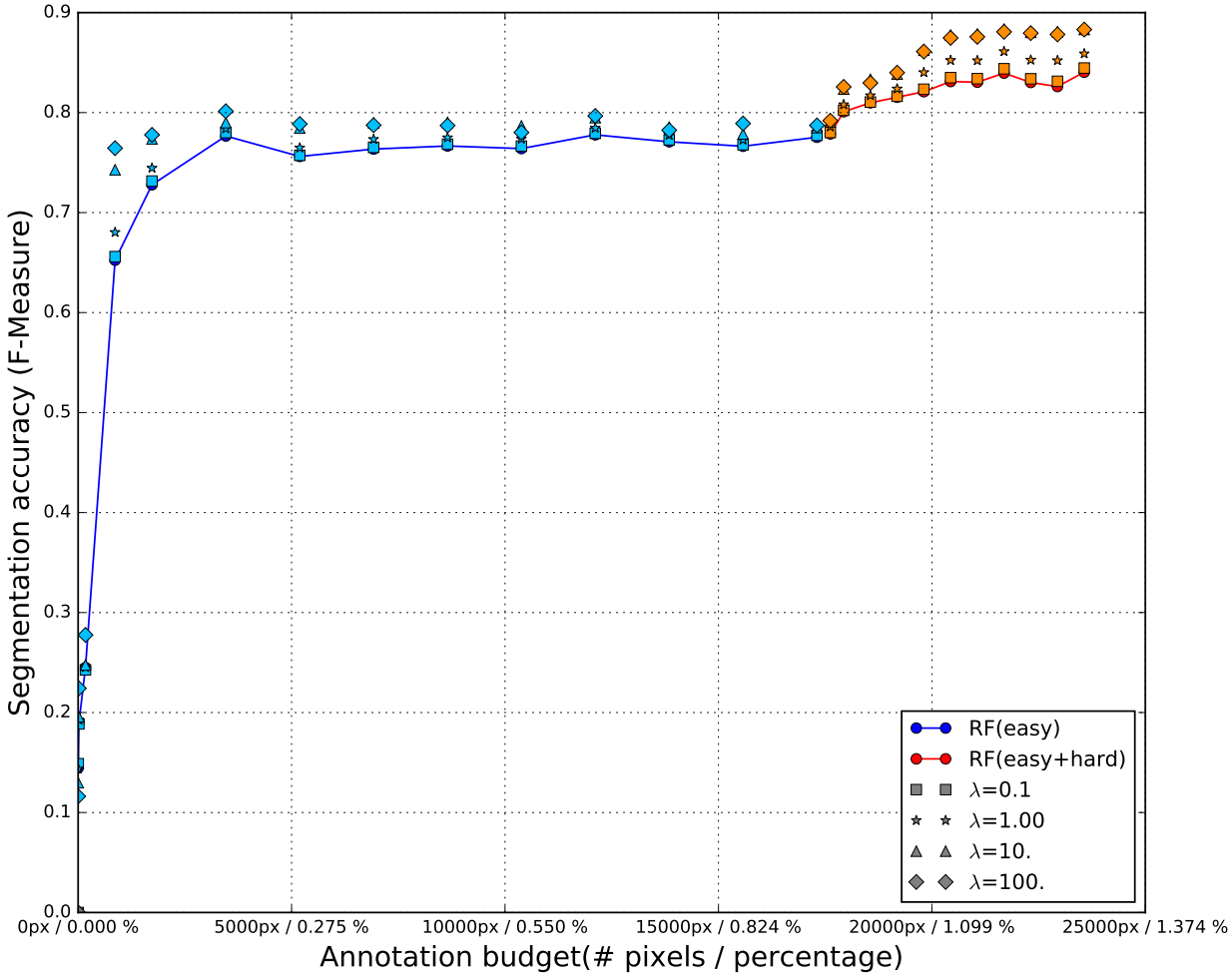

Figure 3.6: Segmentation score with RF and prior(TV) for different annotation budget

function of mask, C_l, as given below:

$$C_l(\boldsymbol{P}) = -4\,(\boldsymbol{P} - 0.5) \quad .$$

We used, ***anit-nll*** cost function, C_{nll}, as given below:

$$C_{nll}(\boldsymbol{P}) = \begin{cases} 0, & \text{if } pixel \in Scribbles \\ -\log \frac{\boldsymbol{P}}{1-\boldsymbol{P}}, & \text{else} \end{cases}$$

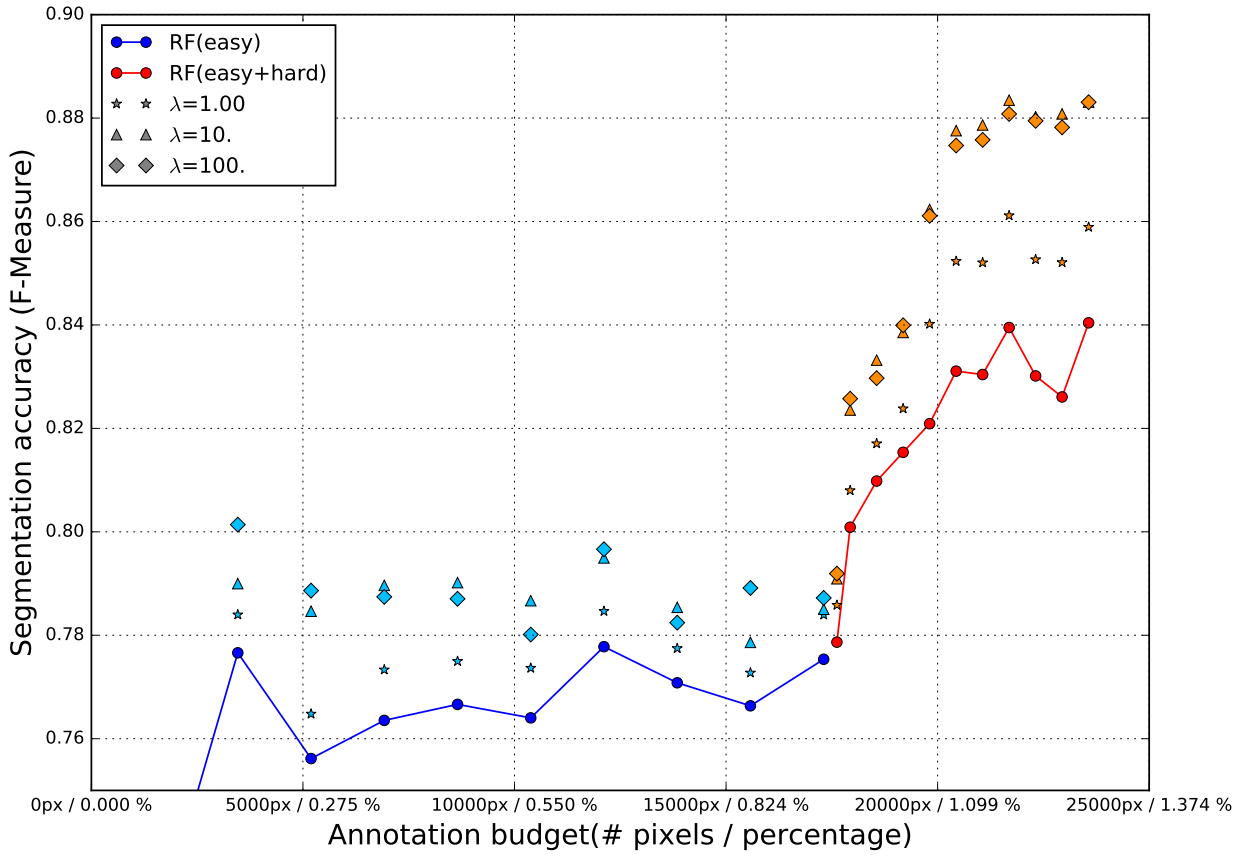

Figure 3.7: Segmentation score with RF and prior(TV) for different annotation budget

For *anti-nll* cost function, we need to use foreground and background constraint for pixel with probability 0 or 1 as we do for scribbles. In addition to the cost function, Santner [5] mentioned use of hard constraint for pixels in foreground or background scribbles i.e. using cost of $-\infty$ for foreground scribbles and ∞ for background scribbles. They didn't show a way to enforce this constraint with *linear* cost function. We enforced this constraint with use of indicator functions.

We used different amount of annotated pixels, randomly selected from ground truth and generated segmentation mask using RF and TV with different cost functions. We generated results to compare 3 cost functions: *linear*, *linear with constraints* and *anti-nll (with constraints)*. The results can be observed in figure 3.8. The *linear* cost function does not work well with large values of λ and also deteriorates the mask obtained from RF. This does not happen with *linear with constraints* and *anti-nll*, where VIP performs always better than RF. This shows robustness of using *linear with constraints* and *anti-nll* cost functions.

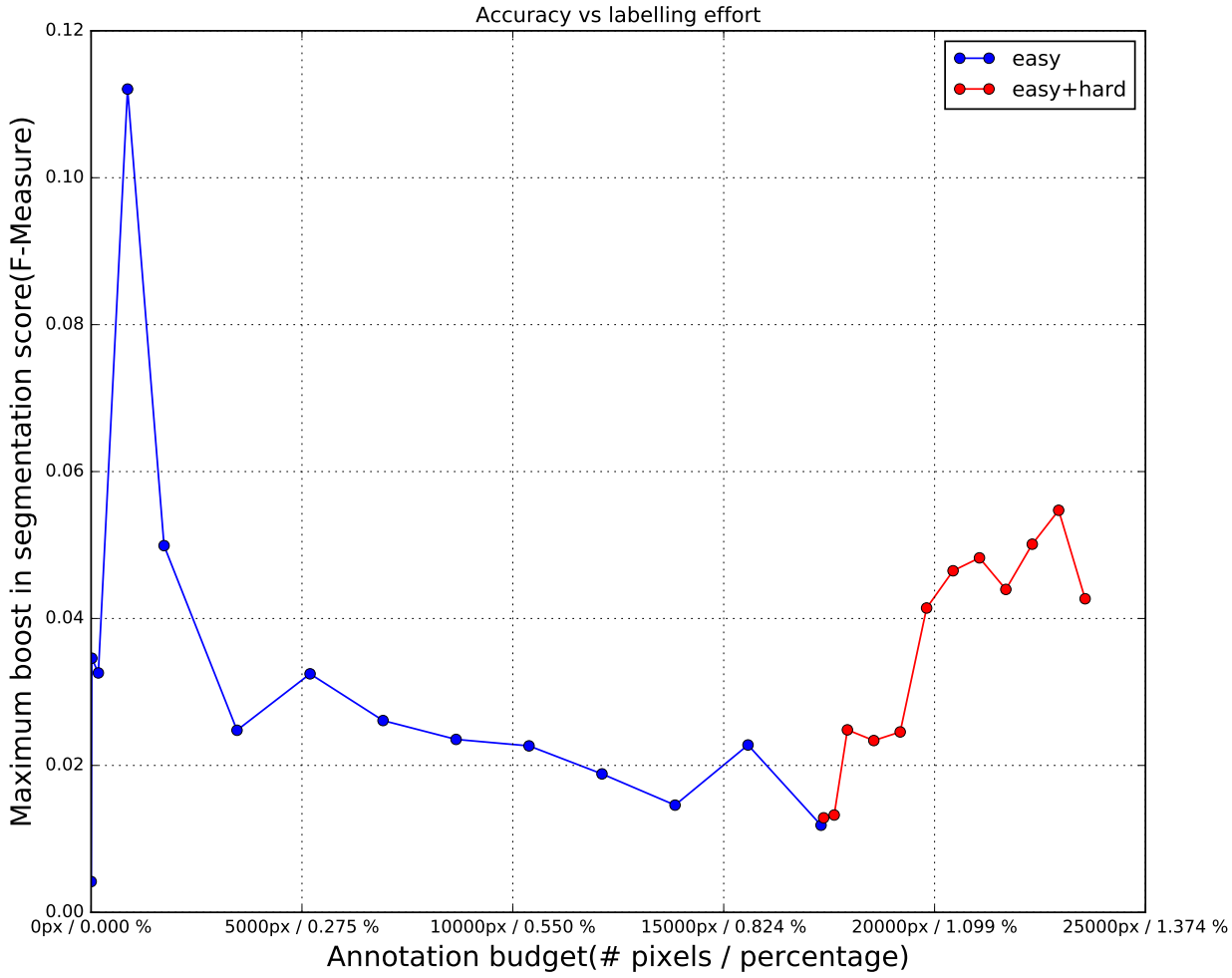

Figure 3.8: Boost obtained with VIP over RF Segmentation score with RF and prior(TV) for different annotation budget

3.2.2 Effect of regularisation parameter

The use of prior information boosts up the performance but we get different boost for different value of λ. The regularisation parameter decides the weight of TV cost. One expects smooth boundaries in segmentation mask for high values, but this also effect mask for small objects. We can observe this in figure 3.9. The upper row shows that for larger vesicles, the boundary gets smooth for higher values of λ, while the bottom row shows that tiny vesicles in image tend to diminish for high values of λ. This shows that the ideal case will be to choose different λ for different part of images or to combine results for different λ.

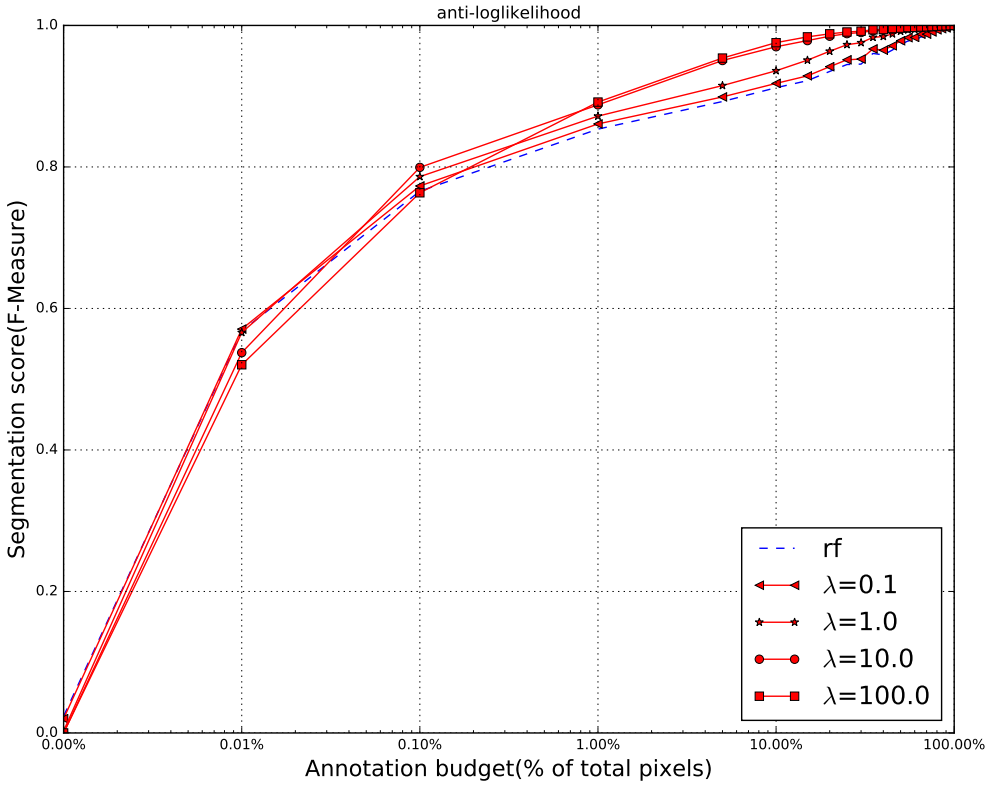

Figure 3.9: VIP with different cost functions

3.3 Semi-interactive segmentation

We realized the need for iterative semi-interactive segmentation in section 3.1.2. With 1 iteration of interactive segmentation, we were able to improve f-measure results. Now, we combine semi-interactive annotation with the use of variational segmentation. We take segmentation mask obtained from variational segmentation and add scribbles to image where the RF and VIP together are unable to segment correctly. Then, we retrain Random forest and generate new mask using variational segmentation. The image, mask, and scribbles are shown in figure 3.10. We can observe the improvement in the mask with an addition of only 5000 pixels (less 0.2% of pixels in the image).

3.4 Training CNN from scribbles

The use of Variational image processing parametrized with cost learned from RF provides a segmentation mask with good accuracy. The RF was trained with features described in WEKA toolset. These features

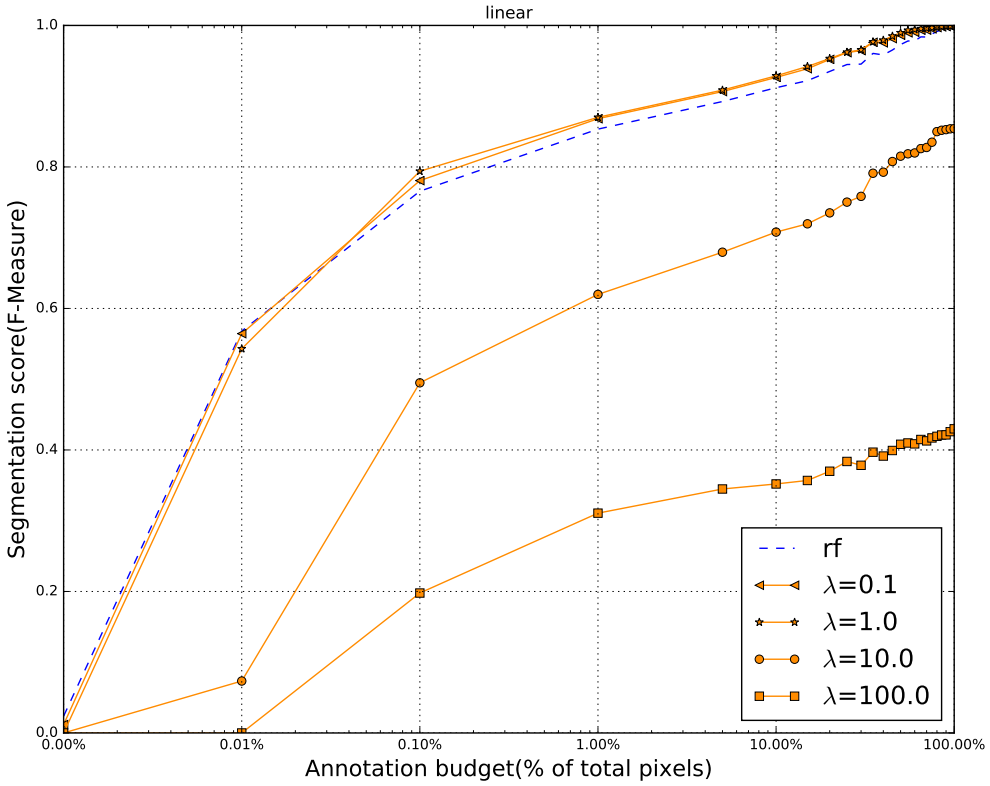

Figure 3.10: VIP with different cost functions

may not work well for certain medical images and thus, use of CNN proves beneficial as it learns different feature maps according to the task. The initial layers learn basic image features while the final layers get trained for filters to compute problem specific results. In addition to this, the choice of λ is always a problem in using VIP. As we showed in section 3.2.2, different parts of images need different values of λ to produce best segmentation mask. Ranftl [6] uses CNN with VIP and modifies the loss function accordingly and learns optimal values of λ along with CNN parameters. The paper describes a method of combining CNN(5 layers) with a final variational/inference layer. The inference layer has activation function in form of Total variation. Similarly, Taylor et al. [14] implemented CNN as a scalable ADMM approach. They split the objective function into subproblems (as we did using ASB) and trained CNN without gradients. These papers attempt to couple CNN with VIP to gain from both approaches.

This motivated us to replace RF with CNN to parametrize cost function. In literature, we can find multiple approaches to train CNN using scribbles. Gonda et al.[15] uses an interactive approach to train deep neural networks for segmentation of neuronal structures using scribbles. Lai et al. [16] uses patch-based

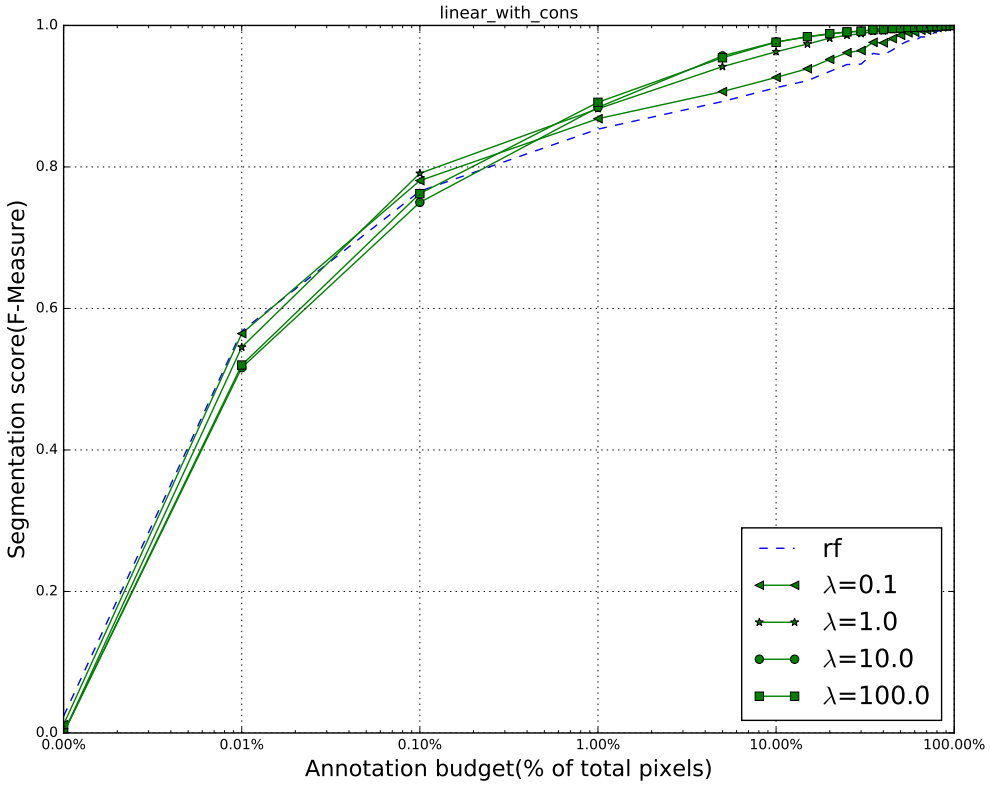

Figure 3.11: VIP with different cost functions

3D image segmentation. They make use of patches around pixels annotated to train the neural network. A similar approach has been used by Havaei et al.[17] for brain tumor segmentation using deep neural networks. These ideas take each pixel as a sample and CNN is trained as a classifier to classify each pixel. The disadvantage is that we remove one major property of CNN to adapt its final layers according to full image for segmentation task and also, it needs sufficient data to train CNN. Therefore, we tried to train OSVOS network (explained in Section 2) from scribbles using **cross entropy scribble loss**. The simple trick we used was to replace computation of cross-entropy loss function for the complete image by computing loss for only annotated scribbles. The **cross entropy scribble loss** can be computed at each pixel, x with probability p, as defined below:

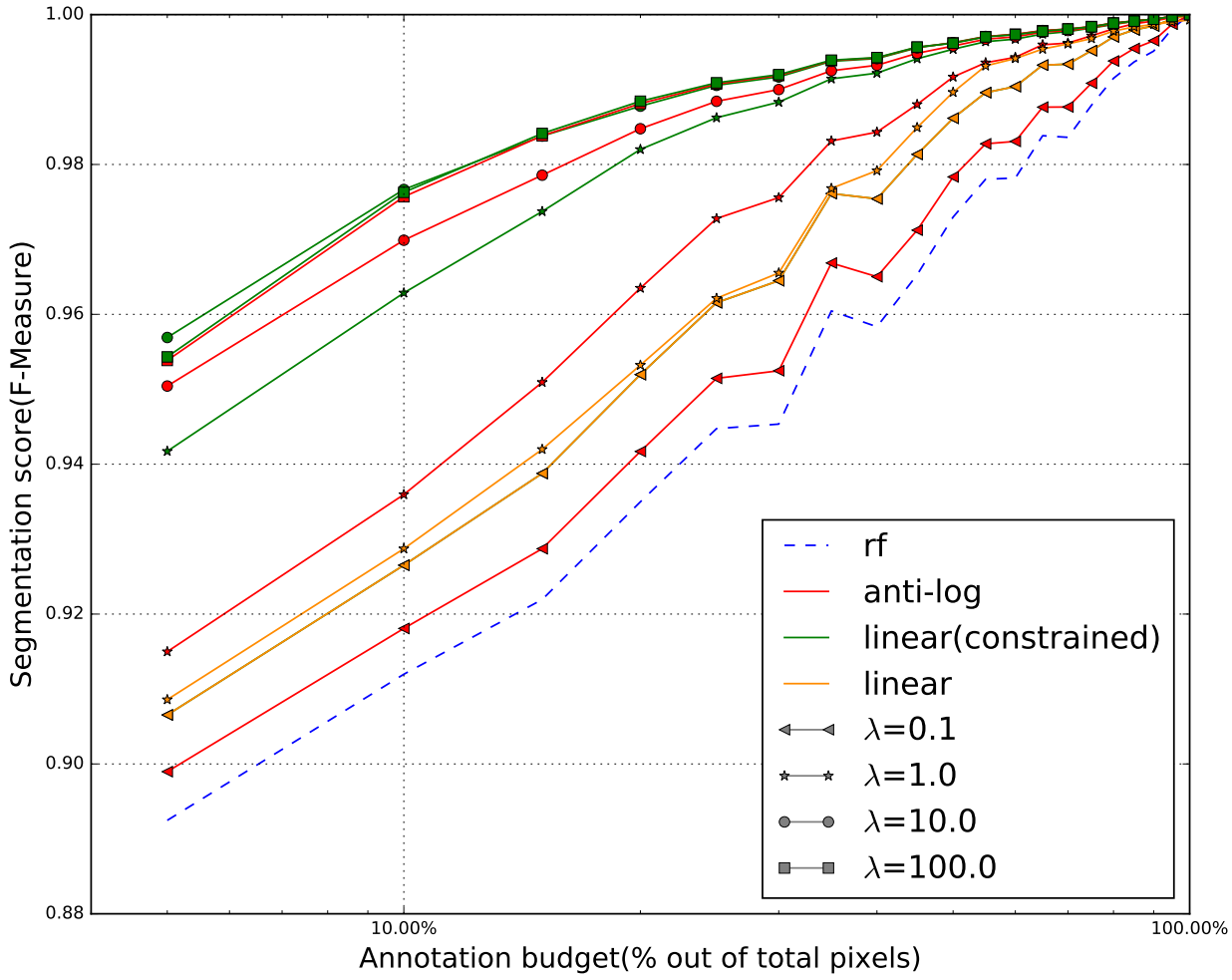

Figure 3.12: VIP with different cost functions

$$l_{scribble}(x) = \begin{cases} -z(x)\,log(p(x)) - (1-z(x))\,log(1-p(x)), & \text{if } x \in \text{Scribbles} \\ 0, & \text{else} \end{cases}$$

We succeeded in training our network with scribble loss and results can be seen in figure 3.11. We compared the results obtained for both RF and CNN using the same amount of pixels annotated. It can be observed that RF looks to perform better for a lower amount of scribbles, while CNN reaches f-measure of a maximum of 0.86 for higher annotation budget. The mask generated using CNN from scribbles shows uncertainity for pixels at boundaries. Thus, we used Variational image processing over mask obtained from

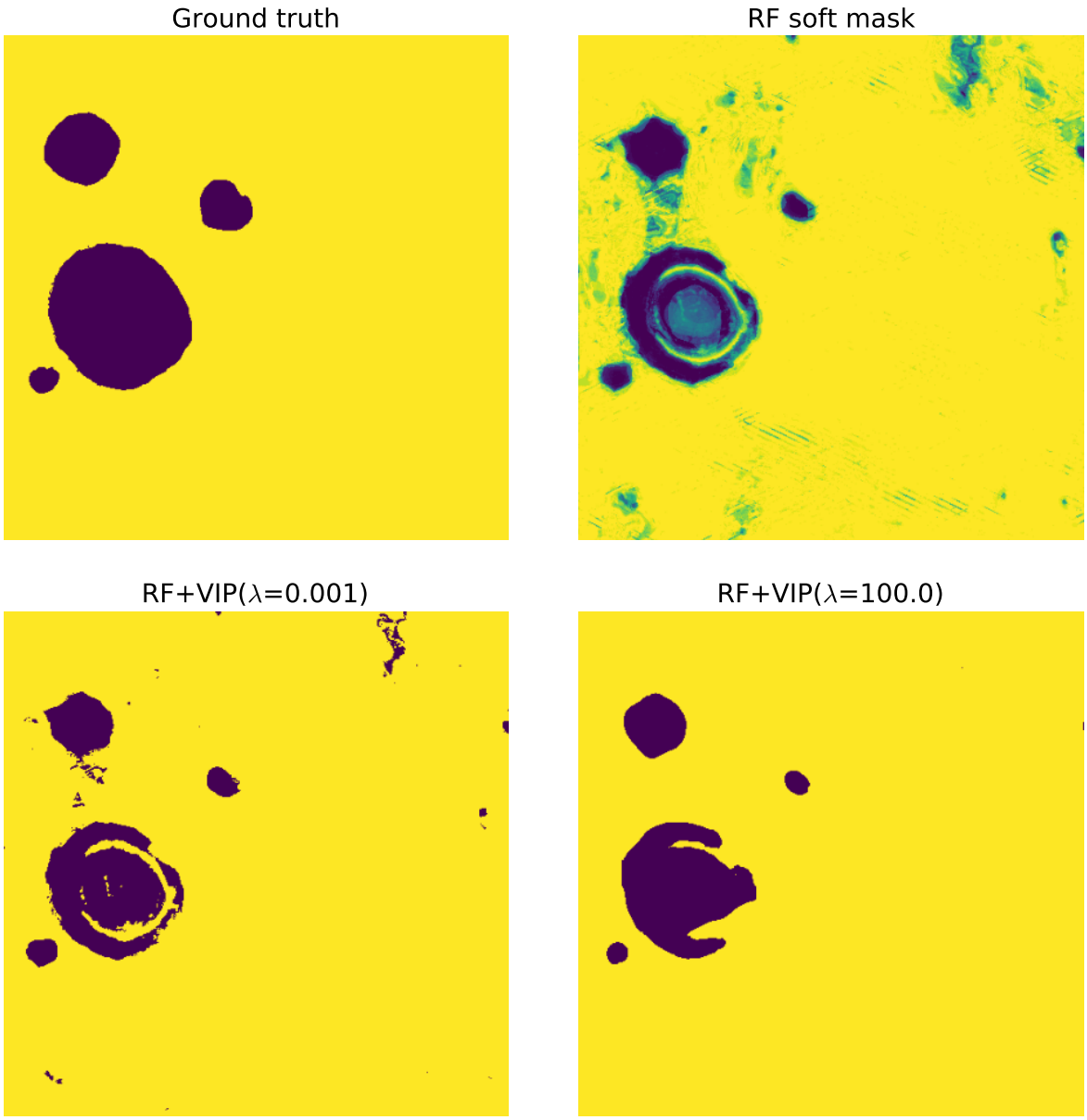

Figure 3.13: Segmentation mask for differnt λ for 2 crops of image

CNN. The boost with VIP can be observed in figure 3.12.

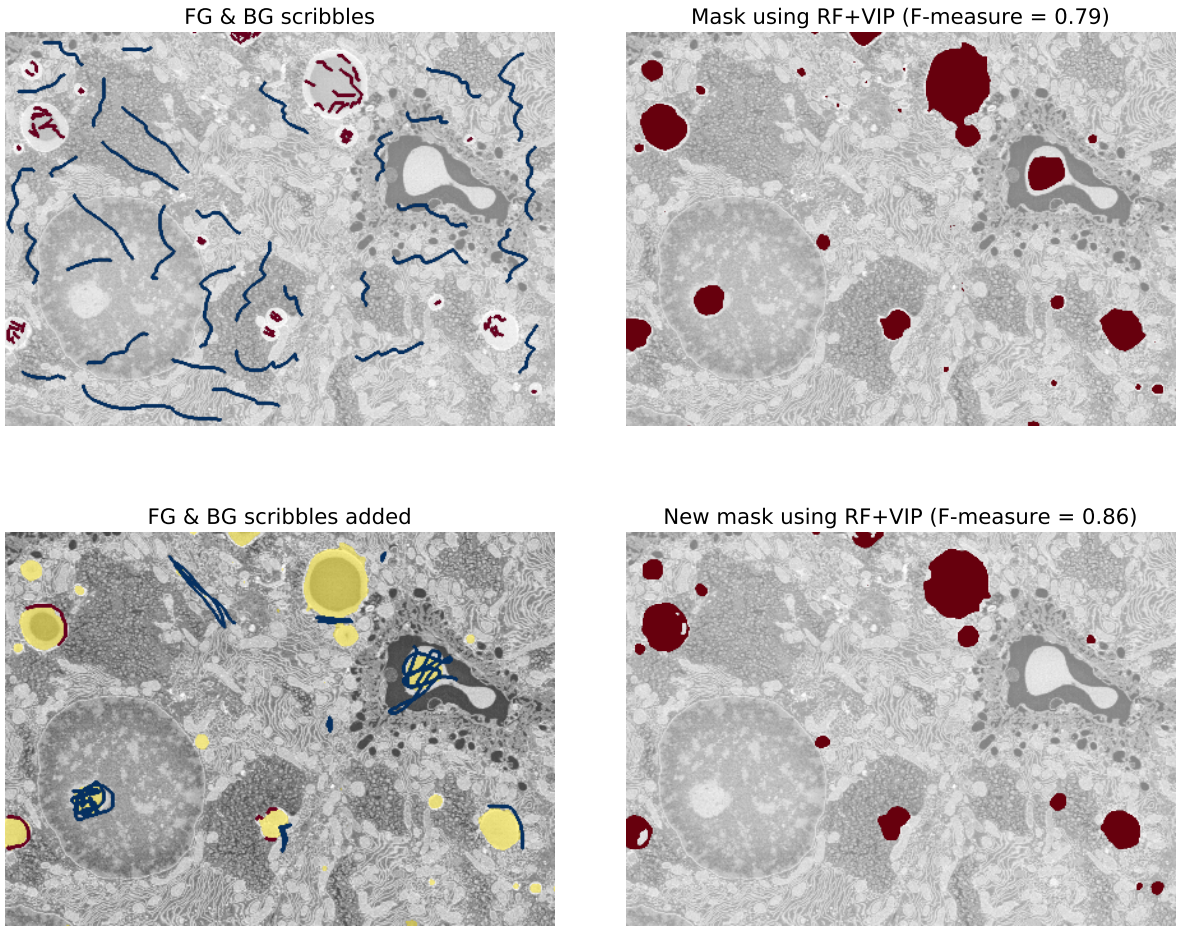

Figure 3.14: Semi-interactive segmentation with one iteration (RF+VIP)

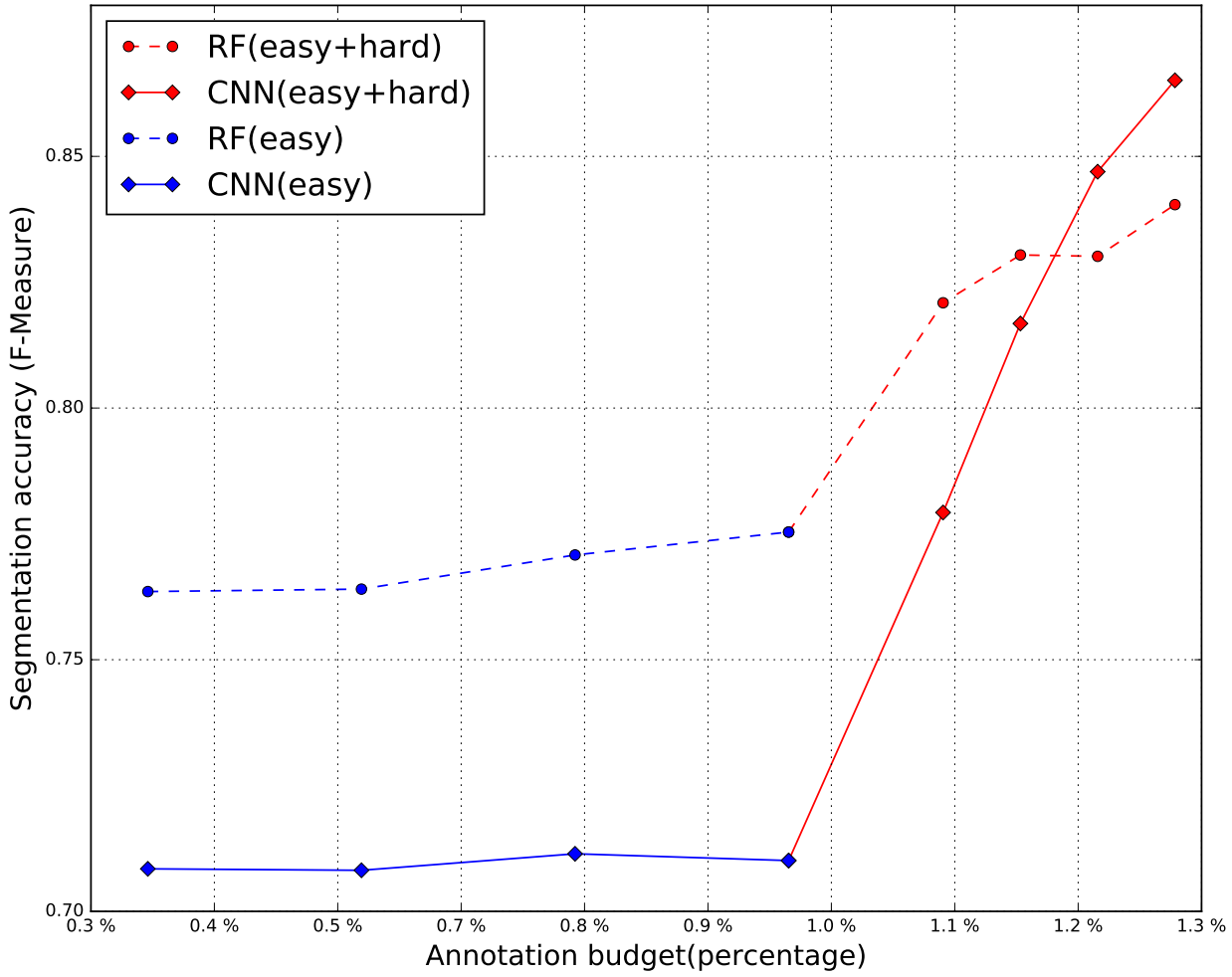

Figure 3.15: F-measure for increasing annotation budget for comparing CNN vs RF

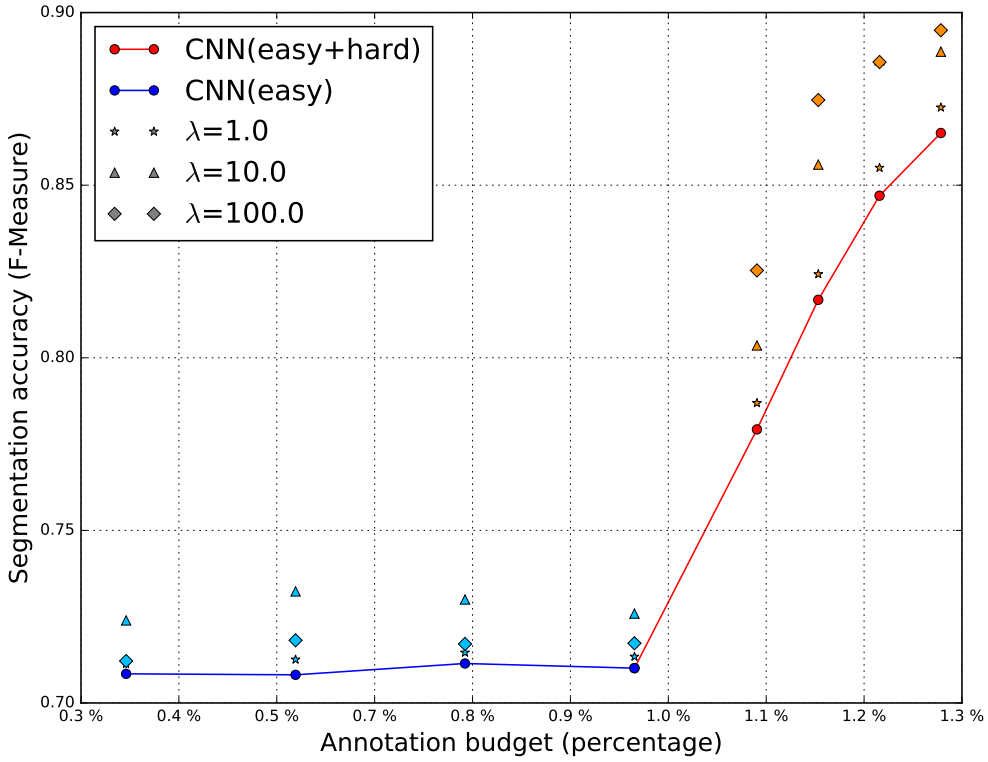

Figure 3.16: (a) CNN with VIP (different λ) (b) CNN vs RF with VIP

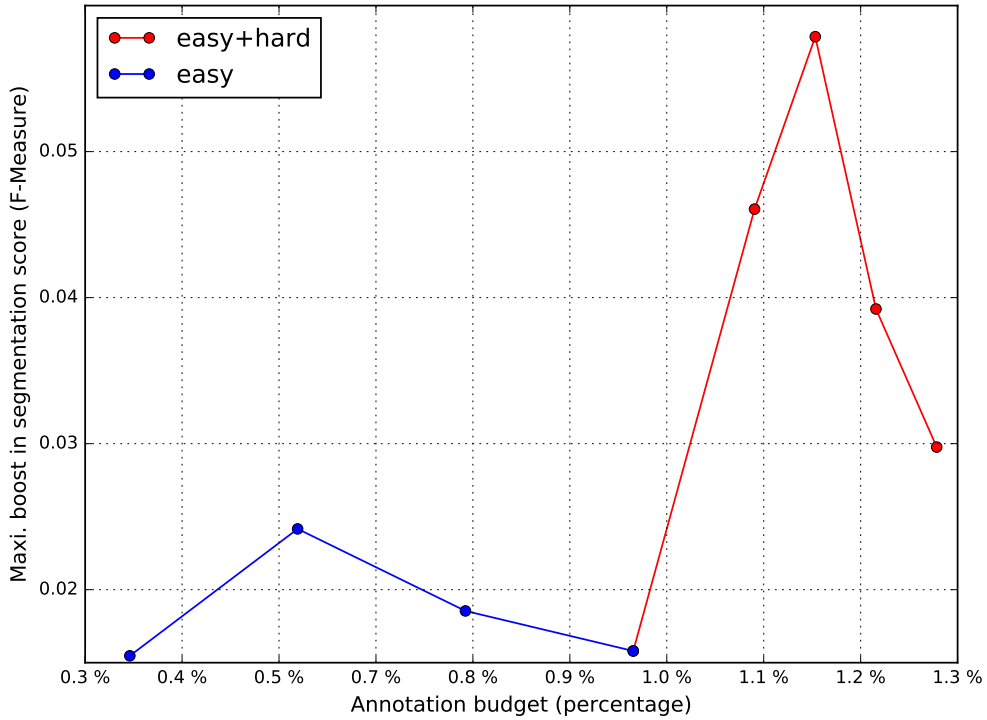

Figure 3.17: (a) CNN with VIP (different λ) (b) CNN vs RF with VIP

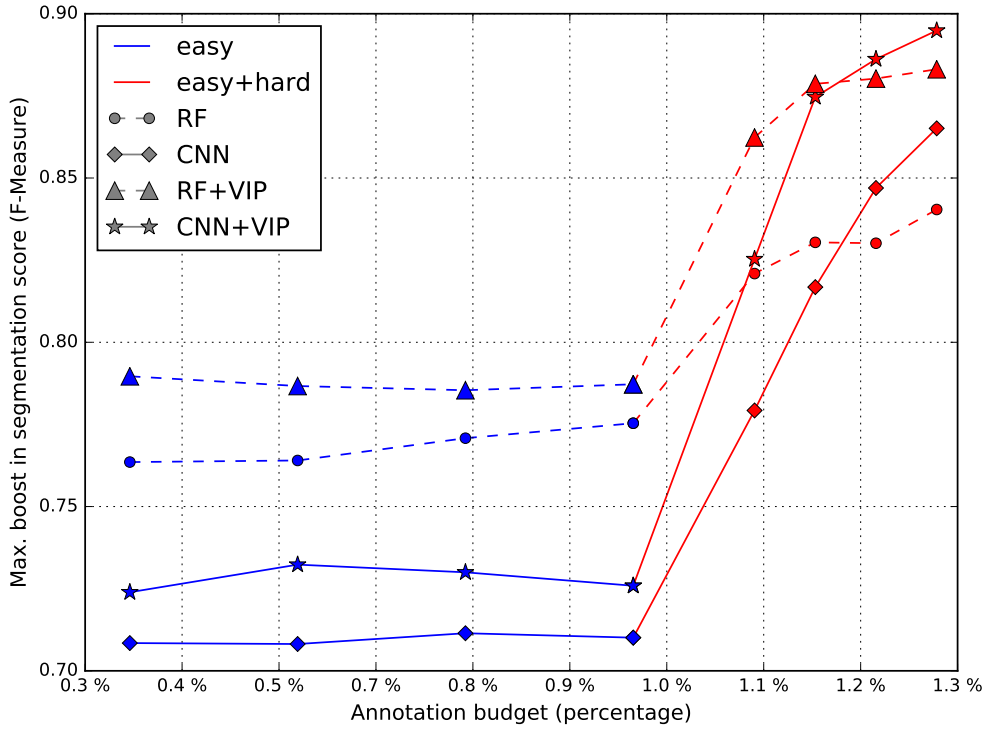

Figure 3.18: (a) CNN with VIP (different λ) (b) CNN vs RF with VIP

Chapter 4

Conclusion

The aim of this thesis was to analyze the relation between segmentation accuracy and annotation effort. We understood the requirement of iterative semi-interactive annotation to obtain best results for given annotation budget. The semi-interactive process can direct us to obtain best results instead of using our effort arbitrarily in semi-supervised learning. Another thing we tried, were different methods to compensate for training data. We started with the use of pre-trained network using fully annotated objects. It was observed to get good results even with 2 images used for training. Then, we used the Bayesian framework to use variational methods and observe a boost in performance. This motivates us to make use of variational methods to compensate for the lack of data. Finally, we were able to use CNN with variational methods to obtain better results. The simple modification of cross entropy loss for scribbles made it possible to use pre-trained fully convolutional networks. This opens a path to use networks pre-trained on million of images in semi-supervised learning. We also observed that for our given data, RF worked better than CNN in the case of fewer data. This can help in making a choice of method to be used for given annotation budget.

Currently, the use of total variation may not be common because of its implementation. It is considered as a post-processing step and not as a solution in a Bayesian framework. In literature, we found recent papers trying to combine CNN and variational methods to obtain better results. They also showed that it can simplify the complexity of CNN and is able to utilize prior information. Ranftl [6] did this by adding total variation as an inference layer and solved the final problem using bilevel optimization [18]. This approach has a benefit to learn appropriate regularization parameter (λ) for total variation. The other approach related

to implementation is to split the iterations used to optimize final problem (mentioned in section 3.2) as separate layers in the neural network. This is termed as Primal-dual network and described in Riegler et al. [8]. Each iteration can be implemented as one additional layer in networks. We tried to couple these two approaches and came up with the idea of having variational neurons similar to convolution filters. These variational neurons will take the image as input and produce a TV regularized output. Instead of learning λ, we can use multiple values of λ and combine then using a CNN. This also opens a way to remove drawback of finding appropriate λ, while using variational methods. Due to time restriction, we were not able to complete this, but this idea can provide an option to get best out of multiple methods in a simple unified way.

Bibliography

[1] O. Ronneberger, P.Fischer, and T. Brox. U-net: Convolutional networks for biomedical image segmentation. In *Medical Image Computing and Computer-Assisted Intervention (MICCAI)*, volume 9351 of *LNCS*, pages 234–241. Springer, 2015. (available on arXiv:1505.04597 [cs.CV]).

[2] Simon K. Warfield, Kelly H. Zou, and William M. Wells. Simultaneous truth and performance level estimation (staple): An algorithm for the validation of image segmentation. *IEEE TRANS. MED. IMAG*, 23:903–921, 2004.

[3] Jonathan Long, Evan Shelhamer, and Trevor Darrell. Fully convolutional networks for semantic segmentation. *CoRR*, abs/1411.4038, 2014.

[4] Sergi Caelles, Kevis-Kokitsi Maninis, Jordi Pont-Tuset, Laura Leal-Taixé, Daniel Cremers, and Luc Van Gool. One-shot video object segmentation. *CoRR*, abs/1611.05198, 2016.

[5] Jakob Santner, Markus Unger, Thomas Pock, Christian Leistner, Amir Saffari, and Horst Bischof. Interactive texture segmentation using random forests and total variation. In *BMVC*, pages 1–12, 2009.

[6] René Ranftl and Thomas Pock. *A Deep Variational Model for Image Segmentation*, pages 107–118. Springer International Publishing, 2014.

[7] Dominic Eugster. Semi-automated 3d object recognition in electron microscopy image data. Master's thesis, 2013.

[8] Gernot Riegler, David Ferstl, Matthias Rüther, and Horst Bischof. A deep primal-dual network for guided depth super-resolution. *CoRR*, abs/1607.08569, 2016.

[9] Gernot Riegler, Matthias Rüther, and Horst Bischof. Atgv-net: Accurate depth super-resolution. *CoRR*, abs/1607.07988, 2016.

[10] Kevis-Kokitsi Maninis, Jordi Pont-Tuset, Pablo Andrés Arbeláez, and Luc J. Van Gool. Deep retinal image understanding. *CoRR*, abs/1609.01103, 2016.

[11] Mark Hall, Eibe Frank, Geoffrey Holmes, Bernhard Pfahringer, Peter Reutemann, and Ian H. Witten. The weka data mining software: An update. *SIGKDD Explor. Newsl.*, 11(1):10–18, November 2009.

[12] J. Schindelin, I. Arganda-Carreras, and E. Frise. Fiji: an open-source platform for biological-image analysis. 9(7):676–682, 2012.

[13] Grégory Paul, Janick Cardinale, and Ivo F. Sbalzarini. Coupling image restoration and segmentation: A generalized linear model/bregman perspective. *International Journal of Computer Vision*, 104(1):69–93, 2013.

[14] Gavin Taylor, Ryan Burmeister, Zheng Xu, Bharat Singh, Ankit Patel, and Tom Goldstein. Training neural networks without gradients: A scalable ADMM approach. *CoRR*, abs/1605.02026, 2016.

[15] Felix Gonda, Ray Thouis Verena Kaynig, Toufiq Parag Daniel Haehn, Jeff Lichtman, and Hanspeter Pfister. Icon: An interactive approach to train deep neural networks for segmentation of neuronal structures. *CoRR*, abs/1610.09032, 2016.

[16] Matthew Lai. Deep learning for medical image segmentation. 2015.

[17] Mohammad Havaei, David Warde-Farley Axel Davy, Aaron C. Courville Antoine Biard, Chris Pal Yoshua Bengio, and Hugo Larochelle Pierre-Marc Jodoin. Brain tumor segmentation with deep neural networks. *CoRR*, abs/1505.03540, 2015.

[18] Peter Ochs, René Ranftl, Thomas Brox, and Thomas Pock. Bilevel optimization with nonsmooth lower level problems. In *International Conference on Scale Space and Variational Methods in Computer Vision*, pages 654–665. Springer, 2015.